The Raman Effect in Crystals

By R. Loudon
Royal Radar Establishment, Malvern, Worcs.

Abstract

A review is given of progress in the theoretical and experimental study of the Raman effect in crystals during the past ten years. Attention is given to the theory of those properties of long-wavelength lattice vibrations in both cubic and uniaxial crystals which can be studied by Raman scattering. In particular the phenomena observed in the Raman scattering from crystals which lack a centre of inversion are related to the theory. The angular variations of the scattering by any type of lattice vibration in a crystal having any symmetry can be easily calculated using a complete tabulation of the Raman tensor. Recent measurements of first-order lattice vibration spectra are listed. A discussion of Brillouin scattering is included. The relation of second-order Raman spectra to critical points in the lattice vibration density of states is discussed, and measurements of the second-order spectra of diamond and the alkali halides are reviewed.

The theory and experimental results for Raman scattering by electronic levels of ions in crystals are examined, and proposals for Raman scattering by spin waves, electronic excitations across the superconductive gap and by plasmons are collected together.

Finally, the prospects for applying lasers as sources for Raman spectroscopy are discussed, and progress in the new technique of stimulated Raman scattering is reviewed.

CONTENTS

§ 1. Introduction

The measurement of the Raman spectrum of a crystal is one of the main methods for obtaining information about its lattice vibration frequencies. The general explanation of the Raman effect has of course been known for a long time; incident light of angular frequency ω_i can interact with the crystal to create or destroy one or more lattice vibration quanta (phonons) and the energy $\hbar\omega$ gained or lost by the lattice is compensated by a decrease or increase in the frequency ω_s of the scattered light ($\omega_s = \omega_i \mp \omega$). However, some of the more subtle effects observed in Raman scattering have only been fully understood within the past ten years with the advent of a more complete knowledge of the properties of lattice vibrations. The purpose of the present article is to review progress in the theory and measurement of the Raman effect during the past decade. For references to earlier work the review article by Menzies (1953) can be consulted. We shall ourselves refer to some of the earlier experimental work, but only where the measurements have been clarified by more recent theoretical analysis or where they are the only measurements on a particularly important substance. Other articles covering particular aspects of the subject have been written during the period under review by Bhagavantam (1953), Mathieu (1956, 1962), and Mitra (1962).

Although many new measurements of Raman spectra have been made during the past ten years, the most striking advances have been in the interpretation of measured spectra in terms of the theory of lattice vibrations, and for this reason a large part of the article is concerned with the theoretical aspects of the subject. As far as the experiments are concerned, most attention is given to the Raman spectra of those crystals whose structure is relatively simple, where theory and experiment can be most easily compared. We shall however give references to measurements on the more complex crystals, although organic crystals are completely excluded. Consideration of the ordinary Raman effect is conveniently divided into two parts; in § 2 we discuss the first-order Raman effect, in which a single phonon is created or destroyed in the scattering process, while § 3 is devoted to the second-order Raman effect, in which two phonons are involved. Raman scattering by excitations of the crystal other than lattice vibrations, e.g. plasmons, spin waves, etc., is dealt with in § 4.

Some falling off in experimental activity is apparent when the work of the past ten years is compared with that in the decade prior to Menzies' review article. Most of the crystals easily obtainable in sufficiently good quality and size, and having strong Raman spectra, were studied in the earlier years and the rate of progress has necessarily slowed down with the more difficult crystals left for investigation. It seems, however, that a new impetus will be given to Raman spectroscopy by the development of the optical maser, or laser. These devices provide powerful collimated beams of monochromatic radiation and appear to be ideal sources for Raman effect measurements. The frequencies of the outputs of presently available lasers extend well below the frequencies of the gas discharge emission lines of sufficient intensity for Raman work, leading to the possibility of measuring the Raman spectra of crystals (e.g. semiconductors) with electronic energy gap smaller than the present minimum of a little over 2 ev. Indeed, lasers may even prove to be more satisfactory sources than gas discharge lamps for all types of crystal. The use of lasers in Raman spectroscopy is discussed in § 5.

§ 2. First-order Raman Effect

2.1. *Properties of Long-wavelength Lattice Vibrations*

The lattice vibrations of the majority of crystals have a maximum wavenumber which varies between about $100\,\mathrm{cm}^{-1}$ and $1000\,\mathrm{cm}^{-1}$ or higher, and first-order Raman spectra occupy a range of this extent on either side of the exciting frequency. The part of the scattered light of lower frequency than the incident light is called the Stokes component, while the part of the scattered light with higher frequency is called the anti-Stokes component. Both optic and acoustic phonons give rise to first-order Raman scattering; we consider first the optic phonons, leaving the acoustic phonons until § 2.7. Only lattice vibrations having certain types of symmetry give rise to Raman scattering; such vibrations are said to be Raman active. The phonon wave vector can take on any value lying in the Brillouin zone, the maximum value being of order π/d, where d is the lattice constant. This maximum is typically of order $3 \times 10^8\,\mathrm{cm}^{-1}$. Incident light with a wavenumber of $20\,000\,\mathrm{cm}^{-1}$ has a wave vector inside the crystal of order $2 \times 10^5\,\mathrm{cm}^{-1}$ (wave vector $= 2\pi \times$ refractive index $\times$ wavenumber) and for scattering of the light through 90°, wave vector conservation requires the wave vector of the phonon created or destroyed to be $\sim \sqrt{2} \times 2 \times 10^5\,\mathrm{cm}^{-1}$. This is small compared to π/d, and the phonons of importance in the first-order Raman effect thus have wavelengths very long compared to the lattice constant.

The smallness of the wave vector $\mathbf{k}$ of the first-order Raman-active phonons leads to a great simplification in the discussion of their properties. There is an important distinction between those lattice vibrations which do or do not produce an electric dipole moment in the lattice, and are thus active or inactive respectively in first-order infra-red absorption. The

frequencies of infra-red-inactive phonons are determined mainly by short-range forces in the lattice; phonons with wavelength long compared to the lattice constant are not influenced by the dispersive effects of these forces and have essentially the same frequency as infinite wavelength phonons. The Raman shifts thus measure the phonon frequencies at $\mathbf{k}=0$, and no variation in the Raman shift is produced by variation of the scattering angle or of the relative orientation of the light beams and the crystal axes. However, for infra-red-active phonons, the accompanying long-range electric fields lead to shifts of the frequencies of some of the Raman-active phonons away from their $\mathbf{k}=0$ values, to a lifting of some of the phonon branch degeneracies, to a variation of frequency with the direction of the phonon wave vector $\mathbf{k}$ in non-cubic crystals, and to other effects which are considered in later sections. A phonon can be simultaneously Raman and infra-red-active only in crystal structures which lack a centre of inversion, i.e. piezo-electric crystals. It is convenient to divide up the discussion of the properties of long-wavelength infra-red-active phonons into three parts corresponding to the three main types of crystal symmetry.

2.1.1. *Cubic crystals*

Huang (1951) has treated the properties of the long-wavelength optic vibrations of a polar diatomic lattice having cubic symmetry (see also Born and Huang 1954). He shows that in the presence of an optic vibration of the lattice having frequency ω, the electric field $\mathbf{E}$ and relative displacement $\mathbf{r}$ of the positive and negative sub-lattices are related by the macroscopic equations:

$$(\omega_0^2-\omega^2)\mathbf{r}=\left(\frac{V}{4\pi M}\right)^{1/2}(\epsilon^0-\epsilon)^{1/2}\omega_0\mathbf{E}, \qquad (1)$$

$$\mathbf{P}=\left(\frac{M}{4\pi V}\right)^{1/2}(\epsilon^0-\epsilon)^{1/2}\omega_0\mathbf{r}+(\epsilon-1)\frac{\mathbf{E}}{4\pi}, \qquad (2)$$

where $\mathbf{P}$ is the polarization, ω_0 is the lattice dispersion frequency, ϵ and ϵ^0 are the optical and static dielectric constants, V is the crystal volume and M is the reduced mass of the two sub-lattices. The effect of anharmonic damping is not included in (1) and (2), and in order for these equations to be valid the inverse phonon relaxation times due to anharmonicity must be small compared to the frequencies of the phonons and the separations between adjacent phonon branches. If the vibration is assumed to have plane-wave form with spatial dependence $\exp(i\mathbf{k}\,.\,\mathbf{R})$, then Maxwell's equations impose the requirement:

$$\mathbf{E}=\frac{-4\pi[\mathbf{k}(\mathbf{k}\,.\,\mathbf{P})-\omega^2\mathbf{P}/c^2]}{k^2-\omega^2/c^2} \qquad (3)$$

All the properties of the long-wavelength optic excitations of the crystal can be derived from (1), (2) and (3). For the transverse solutions,

$\mathbf{k} \cdot \mathbf{P} = 0$, and elimination of $\mathbf{r}$, $\mathbf{E}$ and $\mathbf{P}$ from the equations gives:

$$\frac{k^2c^2}{\omega^2} = \frac{\omega_0^2\epsilon^0 - \omega^2\epsilon}{\omega_0^2 - \omega^2}. \quad . \quad . \quad . \quad . \quad . \quad . \quad . \quad . \quad . \quad (4)$$

For the longitudinal solution $\mathbf{k} \cdot \mathbf{P} = kP$, leading to:

$$\omega = \omega_0\left(\frac{\epsilon^0}{\epsilon}\right)^{1/2} = \omega_l \quad \text{say.} \quad . \quad . \quad . \quad . \quad . \quad . \quad . \quad (5)$$

The schematic form of the ω versus k curves is illustrated in fig. 1, where the numbers in parentheses indicate the branch degeneracy, and L and T denote longitudinal and transverse polarizations. In the region where

Fig. 1

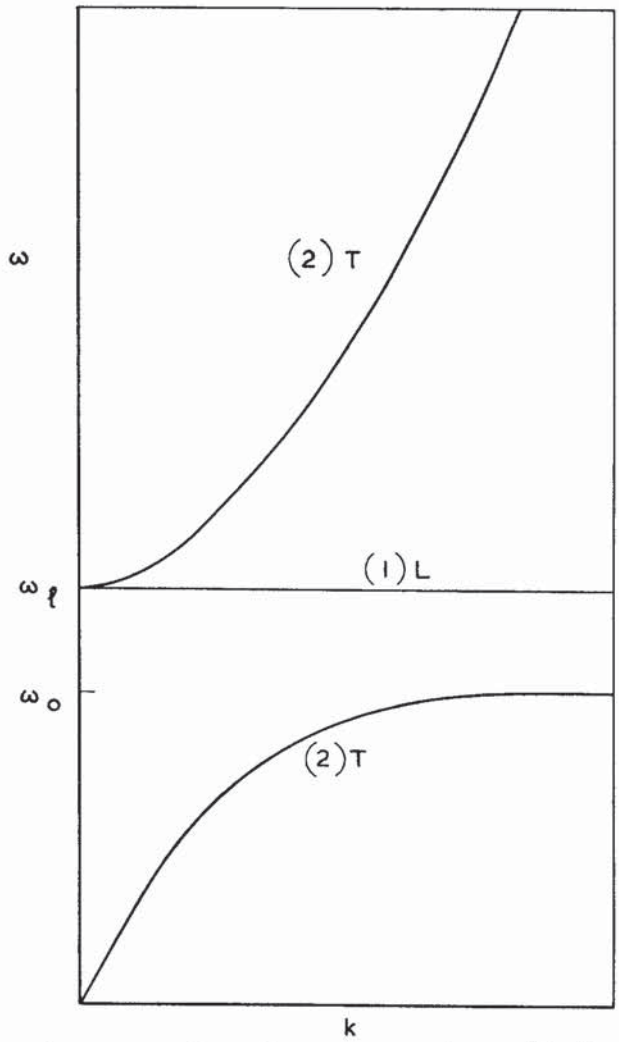

Phonon dispersion curves at small wave vector in a cubic diatomic lattice.

both $\omega < \sim 2\omega_0$ and $k < \sim 2\omega_0(\epsilon^0)^{1/2}/c$, the transverse vibrations are a mixture of lattice oscillation and electromagnetic wave, i.e. the modes are part phonon and part photon. Outside this region, for $\omega > \sim 2\omega_0$ the transverse vibrations are purely photons (modified to some extent by the higher frequency electronic states of the crystal), while the transverse excitations having $\omega = \omega_0$ are purely mechanical oscillations of the lattice having no photon component. Since the phonons which cause right-angle Raman scattering typically have a wave vector $\mathbf{k}$ of order $3 \times 10^5\,\mathrm{cm}^{-1}$ and an angular frequency ω of order $2 \times 10^{14}\,\mathrm{sec}^{-1}$, $\mathbf{k}$ and ω satisfy the inequality $k \gg \omega/c$. The phonons of interest thus lie off the right-hand edge of fig. 1 in the region where the transverse phonons have the constant frequency ω_0. Both the longitudinal and transverse phonons can be Raman active, leading in general to two Stokes and two anti-Stokes peaks in the Raman spectrum, separated from the exciting frequency by amounts of magnitude ω_l and ω_0. The frequencies ω_l and ω_0 are related by (5), a well-known relation first derived by Lyddane *et al.* (1941). At $\mathbf{k} = 0$ the optic branches have a threefold degeneracy with frequency ω_l, although for a finite crystal of dimension L the effect of the long-range electric fields interacting with the sample boundaries may perturb the frequencies of the phonons having wave vector of order, and smaller than $1/L$, and fig. 1 is unreliable in this region.

The electric field strengths associated with the Raman-active phonons can be obtained by substituting the appropriate values of ω into (1). For the transverse phonons, $\omega = \omega_0$ and $E = 0$; for the longitudinal phonons $\omega = \omega_l$ and

$$\mathbf{E} = -\left(\frac{4\pi M}{V}\right)^{1/2} \omega_l \left(\frac{1}{\epsilon} - \frac{1}{\epsilon^0}\right)^{1/2} \mathbf{r}. \qquad (6)$$

The mean square amplitude of the relative sub-lattice displacement $\mathbf{r}$ due to a lattice vibration of frequency ω is:

$$\langle r^2 \rangle = (2n+1)\hbar/2M\omega, \qquad (7)$$

where n is the number of phonons contributing to the vibration; in thermal equilibrium:

$$n = [\exp(\hbar\omega/k_B T) - 1]^{-1}, \qquad (8)$$

where k_B is Boltzmann's constant and T is the temperature.

The above theory applies directly to a polar diatomic lattice; the zinc blende structure is an example of a crystal with two atoms in the unit cell whose optic vibrations are both Raman and infra-red active. For crystals with more than two atoms in the unit cell but still having only one infra-red-active vibration (e.g. CaF_2), the results continue to hold, but where more than one vibration is infra-red active the theory must be extended. We do not pursue this case in any detail, except to quote an extension of the Lyddane–Sachs–Teller relation (5) due to Cochran and Cowley (1962). This applies in its most general form to a crystal of any symmetry having any number of infra-red-active branches. For a cubic

crystal having N infra-red-active vibrations with longitudinal and transverse frequencies $\omega_L(j)$ and $\omega_T(j)$ ($j=1, 2, \ldots N$) the generalization of (5) is:

$$\prod_{j=1}^{N}\left[\frac{\omega_L(j)}{\omega_T(j)}\right]^2 = \frac{\epsilon^0}{\epsilon} \quad . \quad . \quad . \quad . \quad . \quad . \quad . \quad . \quad . \quad (9)$$

2.1.2. *Uniaxial crystals*

Merten (1960) and Loudon (1963 a) have treated some of the properties of long-wavelength lattice vibrations in uniaxial crystals. The treatment is based on a generalization of Huang's equations for a cubic crystal given in the previous sub-section. We consider a uniaxial crystal in which only one group of three lattice vibration branches is infra-red active, for example the wurtzite structure. Due to the anisotropy of the crystal, in the absence of long-range electric forces the vibration in which the atoms are displaced parallel to the c-axis has a frequency $\omega_\parallel$ which is different to the frequency $\omega_\perp$ of the two degenerate vibrations in which the atomic displacements lie perpendicular to the c-axis, in the ab-plane. The number of high and low frequency dielectric constants is correspondingly doubled. The phonon spectrum is obtained by writing down pairs of equations similar to (1) and (2) for the components of oscillation parallel and perpendicular to the c-axis. Equation (3) continues to hold since it is derived directly from Maxwell's equations, with no assumptions about the crystal structure; it can be divided into two equations for the components of **E** parallel and perpendicular to the c-axis. This gives a total of six equations, enabling elimination of the two components each of **r**, **P** and **E**. For any relative orientation of the phonon wave vector **k** and the c-axis, the equations have a solution in which **E** and **P** are perpendicular to both **k** and the c-axis. This corresponds to the ordinary wave, and leads to:

$$\frac{k^2c^2}{\omega^2} = \frac{\omega_\perp^2\epsilon_\perp^0 - \omega^2\epsilon_\perp}{\omega_\perp^2 - \omega^2} \quad \text{(ordinary wave).} \quad . \quad . \quad . \quad (10)$$

The other solutions correspond to the extraordinary waves, and **E** and **P** do not in general have any simple orientation relative to **k** and the c-axis (although the displacement **D** is perpendicular to **k**). The frequencies of the extraordinary waves depend on the angle θ between **k** and the c-axis:

$$\frac{k^2c^2}{\omega^2} = \frac{\left[\frac{\omega_\parallel^2\epsilon_\parallel^0 - \omega^2\epsilon_\parallel}{\omega_\parallel^2 - \omega^2}\right]\left[\frac{\omega_\perp^2\epsilon_\perp^0 - \omega^2\epsilon_\perp}{\omega_\perp^2 - \omega^2}\right]}{\left[\frac{\omega_\parallel^2\epsilon_\parallel^0 - \omega^2\epsilon_\parallel}{\omega_\parallel^2 - \omega^2}\right]\cos^2\theta + \left[\frac{\omega_\perp^2\epsilon_\perp^0 - \omega^2\epsilon_\perp}{\omega_\perp^2 - \omega^2}\right]\sin^2\theta}$$

(extraordinary waves). . . (11)

Notice that for $\theta = 0$ (propagation parallel to the c-axis) (11) reduces to (10), and that (11) reduces to (4) when the distinction between $\parallel$ and $\perp$ quantities is removed.

It is convenient to define two frequencies:

$$\omega_\parallel^l = \omega_\parallel\left(\frac{\epsilon_\parallel^0}{\epsilon_\parallel}\right)^{1/2} \quad \text{and} \quad \omega_\perp^l = \omega_\perp\left(\frac{\epsilon_\perp^0}{\epsilon_\perp}\right)^{1/2} \quad . \quad . \quad . \quad . \quad (12)$$

analogous to ω_l defined by (5) for cubic crystals. Reference to (10) and (11) shows that for $\mathbf{k}=0$ the phonon frequencies are $\omega_{\|}^l$ (singlet) and $\omega_{\perp}^l$ (doublet). The Raman-active vibrations have $k \gg \omega/c$ as before, and (10) and (11) show that the Raman frequencies are given by:

and $$\omega = \omega_{\perp} \quad \text{(ordinary phonon)}, \qquad \ldots \quad (13)$$

$$\left[\frac{\omega_{\|}^2 \epsilon_{\|}^0 - \omega^2 \epsilon_{\|}}{\omega_{\|}^2 - \omega^2}\right] \cos^2\theta + \left[\frac{\omega_{\perp}^2 \epsilon_{\perp}^0 - \omega^2 \epsilon_{\perp}}{\omega_{\perp}^2 - \omega^2}\right] \sin^2\theta = 0 \quad \text{(extraordinary phonons)}. \qquad \ldots \quad (14)$$

Equation (14) is a quadratic for ω^2, having in general two distinct roots, and the ordinary and extraordinary phonons together contribute three Stokes (and three anti-Stokes) lines to the Raman spectrum, except for certain special orientations of the crystal. If ω_1^2 and ω_2^2 are the two roots of (14), it is easy to show that they satisfy a modified Lyddane–Sachs–Teller relation:

$$\frac{\omega_1^2 \omega_2^2}{\omega_{\|}^2 \omega_{\perp}^2} = \frac{\epsilon_{\|}^0 \cos^2\theta + \epsilon_{\perp}^0 \sin^2\theta}{\epsilon_{\|} \cos^2\theta + \epsilon_{\perp} \sin^2\theta}. \qquad \ldots \quad (15)$$

The electric field strength associated with a Raman-active phonon is given by the generalizations of (1) with the appropriate value of ω substituted. The ordinary phonon has zero electric vector and so also does an extraordinary phonon when θ is such as to make its frequency either $\omega_{\|}$ or $\omega_{\perp}$ (this can occur only for $\theta = 0$ or $90°$). Equation (3) shows that $\mathbf{E}$ is parallel to $\mathbf{k}$ for the extraordinary phonons (when $k \gg \omega/c$).

Rather than discuss (14) for general values of the frequencies and dielectric constants, it is more convenient to consider two limiting cases which correspond to many crystals of experimental interest.

(i) $|\omega_{\|} - \omega_{\perp}| \ll \omega_{\|}^l - \omega_{\|}$ and $\omega_{\perp}^l - \omega_{\perp}$. In this case, the difference in frequency of vibrations parallel and perpendicular to the c-axis, caused by anisotropy of the force constants, is small compared to the difference between the frequencies with and without the l superscript, which is caused by electrostatic forces. Hexagonal ZnO and SiC are examples of crystals where this limit holds (see § 2.6). For $\theta = 0$ the two solutions of (14) are $\omega_{\perp}$ and $\omega_{\|}^l$, while for $\theta = 90°$ the solutions are $\omega_{\|}$ and $\omega_{\perp}^l$. For general values of θ, one root of (14) lies in the vicinity of $\omega_{\|}$ and $\omega_{\perp}$ while the second root is close to $\omega_{\|}^l$ and $\omega_{\perp}^l$. Using the assumed inequalities satisfied by the characteristic frequencies and assuming, in addition that the percentage difference between $\epsilon_{\|}$ and $\epsilon_{\perp}$ is small, the two solutions of (14) are approximately:

$$\omega^2 = \omega_{\|}^2 \sin^2\theta + \omega_{\perp}^2 \cos^2\theta \qquad \ldots \quad (16)$$

and

$$\omega^2 = \omega_{\|}^{l^2} \cos^2\theta + \omega_{\perp}^{l^2} \sin^2\theta. \qquad \ldots \quad (17)$$

The complete dispersion curves in this limit are plotted in fig. 2 for three directions of propagation. The relative values of the frequencies and dielectric constants have been chosen arbitrarily for a negative uniaxial

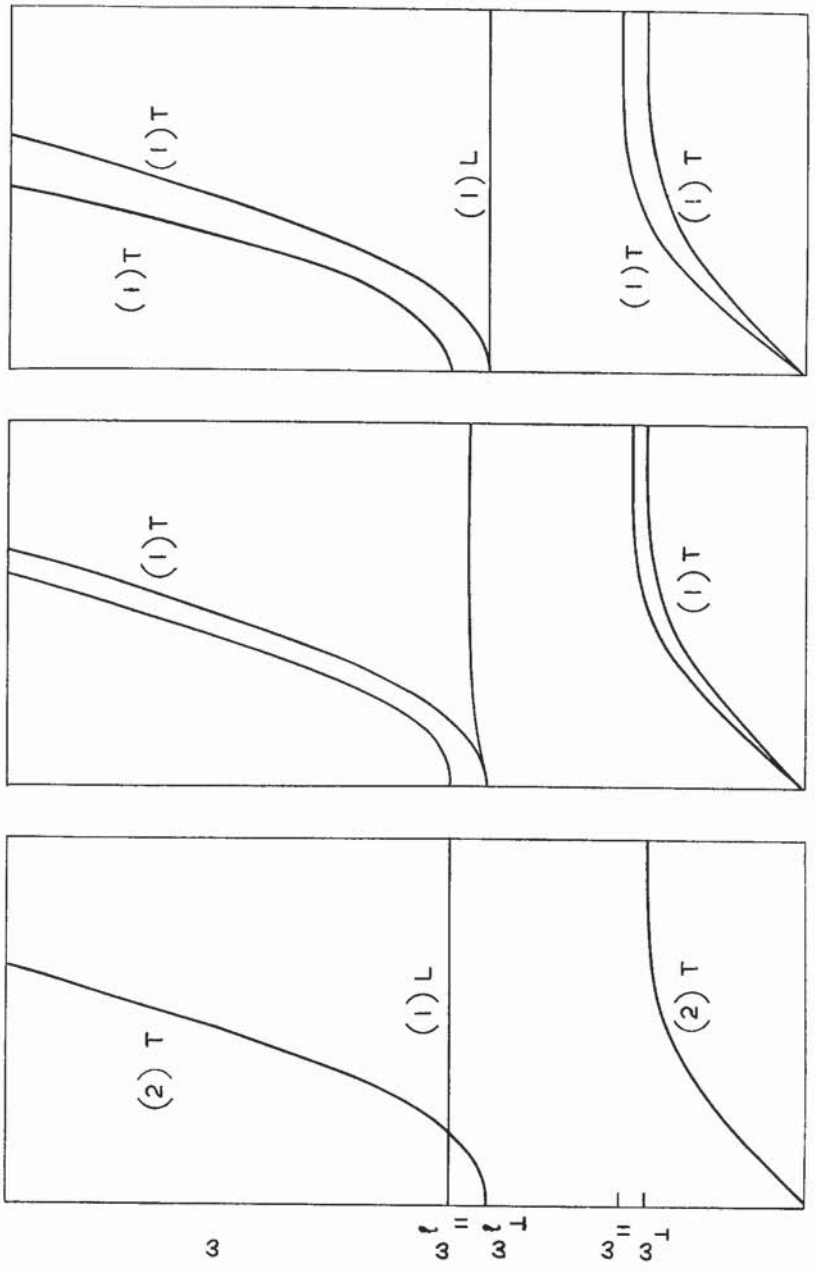

Fig. 2

Phonon dispersion curves at small wave vector in a uniaxial crystal for which electrostatic forces predominate over anisotropy in the interatomic forces. Phonon wave vector (*a*) parallel to *c*-axis, (*b*) in intermediate direction and (*c*) lying in the *ab*-plane.

crystal. The frequencies of the Raman-active phonons given by (13) and (14), and approximately by (16) and (17), are associated with the phonons at the right-hand edges of the graphs where the branches are flat. The extraordinary branches have strictly no simple polarization except for $\theta = 0$ and $90°$. However the predominance of electrostatic forces over the anisotropy in the interatomic forces ensures that the departures of the upper phonon branch from longitudinal polarization, and of the lower branch from transverse polarization, are small. The electric field associated with the upper branch is of the same order as that in cubic crystals given by (6), while the electric field associated with the lower branch is much smaller, roughly by a factor $[(\omega_{\|}^2 - \omega_{\perp}^2)/(\omega_{\|}^{l2} - \omega_{\|}^2)]$. The anisotropy in the infra-red properties of this type of crystal is small.

(ii) $|\omega_{\|} - \omega_{\perp}| \gg \omega_{\|}^l - \omega_{\|}$ and $\omega_{\perp}^l - \omega_{\perp}$. For this case, one solution of (14) always lies in the vicinity of $\omega_{\|}$ and $\omega_{\|}^l$ and the other solution always lies in the vicinity of $\omega_{\perp}$ and $\omega_{\perp}^l$. Approximate solutions of (14), obtained as before, are:

$$\omega^2 = \omega_{\|}^2 \sin^2\theta + \omega_{\|}^{l2} \cos^2\theta, \quad . \quad . \quad . \quad . \quad . \quad . \quad (18)$$

$$\omega^2 = \omega_{\perp}^2 \cos^2\theta + \omega_{\perp}^{l2} \sin^2\theta. \quad . \quad . \quad . \quad . \quad . \quad . \quad (19)$$

Dispersion curves in this limit for three directions of propagation are plotted in fig. 3. As θ is increased from 0 to $90°$, the upper extraordinary branch changes from longitudinal to transverse polarization, while the lower branch changes from transverse to longitudinal. For intermediate values of θ the extraordinary branches have strictly no simple polarization, although the predominance of the anisotropy in the interatomic forces over the long-range electric forces causes the relative sub-lattice displacement $\mathbf{r}$ in the upper phonon branch to be almost parallel to the c-axis, with the displacement in the lower branch approximately perpendicular to the c-axis, for all values of θ. Since only a transversely polarized phonon can be infra-red active, there is considerable anisotropy in the infra-red properties of this type of crystal.

Formulae equivalent to (18) and (19) were first derived by Poulet (1952, 1955), and Ketelaar *et al.* (1954) have given a theory of the variation with θ of the intensity and frequency of the reflection from a uniaxial crystal. Observations of the variation with θ of the frequency of the maximum of a reflection band have been made by Couture-Mathieu *et al.* (1952 a, b) on crystals of quartz, lithium perchlorate ($LiClO_4 . 3H_2O$) and iodic acid (IO_3H). All these crystals appear to satisfy the frequency inequality assumed in this sub-section, although the inequality is only weakly satisfied in the case of quartz. In any case, the maximum in the reflection band does not occur exactly at the phonon frequency ω, so that the above measurements cannot be closely related to the theory without more detailed calculations of the shape of the reflection band. Some progress in this direction has been made by Ketelaar *et al.* (1954) who compared their theory with experiments on sodium nitrate ($NaNO_3$). A much more direct comparison of the theory of this section with experiment can be made for

Fig. 3

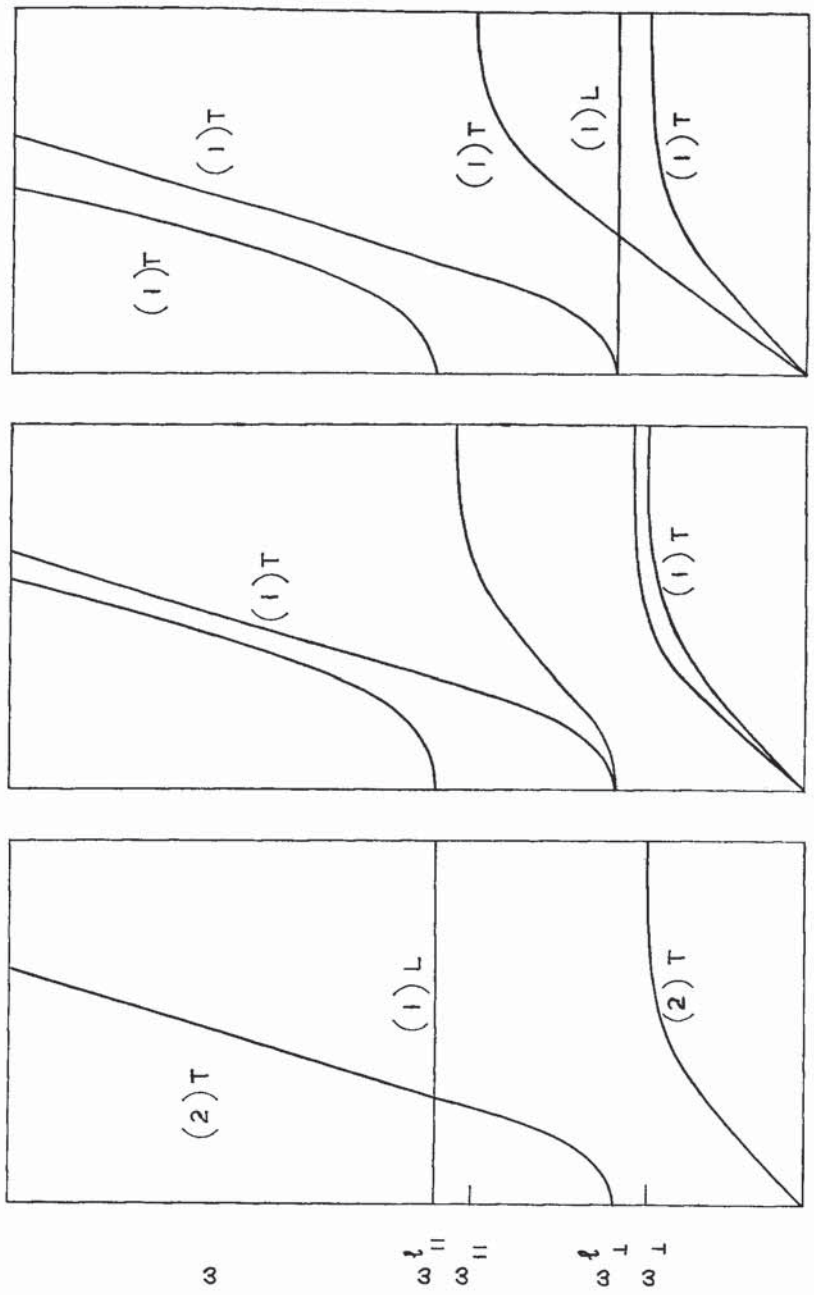

Phonon dispersion curves at small wave vector in a uniaxial crystal for which anisotropy in the interatomic forces predominates over electrostatic forces. Phonon wave vector (*a*) parallel to *c*-axis, (*b*) in intermediate direction and (*c*) lying in the *ab*-plane.

the results on the variation of Raman frequency with θ (see § 2.6). Mention may also be made of the work of Tramer (1959 a, b), who observed the variation of phonon frequency with θ in sodium nitride ($NaNO_2$) by direct absorption measurements as well as by the Raman effect. Reviews of the relevant infra-red and Raman results in this field have been given by Haas (1956) and Mathieu *et al.* (1960).

Expressions for the electric fields associated with the upper and lower phonon branches in fig. 3 can be derived from the generalizations of (1), (2) and (3), using (12), (18) and (19):

$$\mathbf{E} = -\left(\frac{4\pi M}{V}\right)^{1/2} \omega_{\parallel}^{l} \cos\theta \left(\frac{1}{\epsilon_{\parallel}} - \frac{1}{\epsilon_{\parallel}^{0}}\right)^{1/2} r_{\parallel} \hat{\mathbf{k}} \quad \text{(upper branch)}, \quad . \quad (20)$$

$$\mathbf{E} = -\left(\frac{4\pi M}{V}\right)^{1/2} \omega_{\perp}^{l} \sin\theta \left(\frac{1}{\epsilon_{\perp}} - \frac{1}{\epsilon_{\perp}^{0}}\right)^{1/2} r_{\perp} \hat{\mathbf{k}}, \text{ (lower branch)}, \quad . \quad (21)$$

where $r_{\parallel}$ and $r_{\perp}$ are the components of $\mathbf{r}$ parallel and perpendicular to the c-axis and $\hat{\mathbf{k}}$ is a unit vector parallel to $\mathbf{k}$. These values for the field strength will be used in calculating the Raman scattering intensity. Expressions equivalent to (20) and (21) have been derived by Poulet (1955). Our choice for the relative magnitude of $\omega_{\parallel}$ and $\omega_{\perp}$ is of course arbitrary; for many crystals $\omega_{\parallel}$ is smaller than $\omega_{\perp}$.

The theory of this sub-section ceases to be valid when more than one group of three lattice vibrations is infra-red active. There is little theoretical work on the properties of the lattice vibrations in this situation, although the generalizations of the Lyddane–Sachs–Teller relation due to Cochran and Cowley (1962) continue to apply. For a group of infra-red-active phonons which is well separated from the remaining groups, the variations of their frequencies with θ may still be represented by equations similar to (18) and (19), but the constants occurring in them are not related to the dielectric constants by (12).

2.1.3. *Biaxial crystals*

There is little work, either theoretical or experimental, on the Raman effect in biaxial crystals. The long-wavelength properties could be determined by writing down equations similar to (1) and (2) for the components of oscillation in the directions of the three principal axes. The frequencies of the three Raman-active phonons are determined by a cubic equation in ω^2 and they all vary with direction of propagation.

2.2. *Theory of the Scattering Process*

Each elementary Raman scattering event involves the destruction of a photon of frequency ω_i, incident from a light source, the creation of a scattered photon of frequency ω_s, and the creation or destruction of a phonon of frequency ω. We choose to concentrate on the Stokes component of the scattering, so that $\omega_i = \omega_s + \omega$; the properties of the anti-Stokes

component can always be obtained by simple substitutions. Figure 4 illustrates three different Raman scattering processes in terms of the elementary interactions between the radiation, the electrons and the lattice; H_{EL}, $H_{RL}^{(1)}$ and H_{ER} represent, in an obvious notation, the first-order interactions between the three systems. The three-phonon anharmonic interaction H_A and the second-order moment radiation-lattice interaction $H_{RL}^{(2)}$ (see Lax and Burstein 1955) are higher-order interactions.

Fig. 4

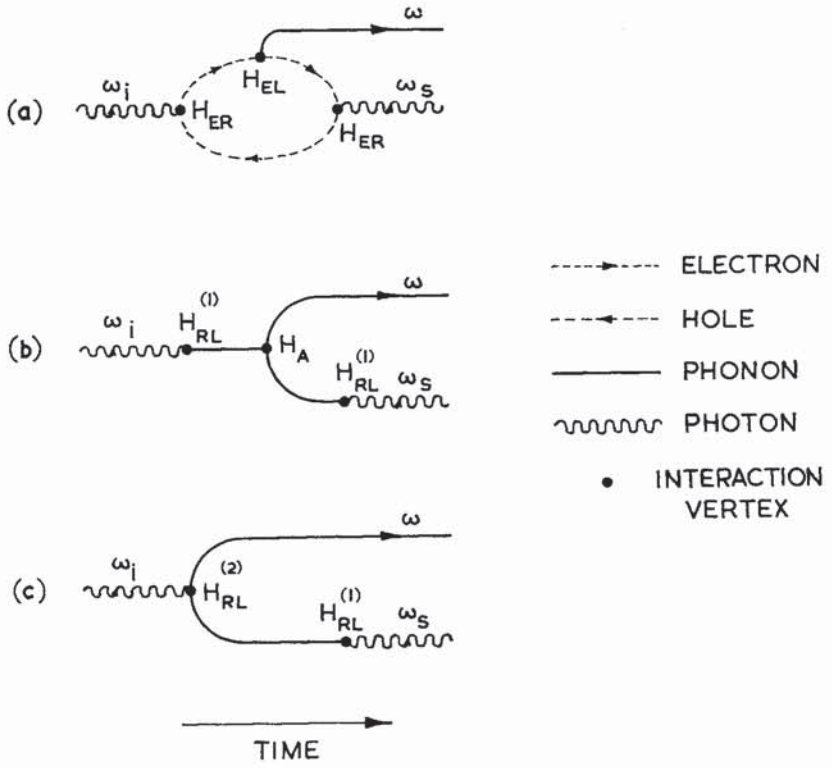

Three types of elementary Raman scattering process.

The initial state, with photon ω_i present, occurs at the left-hand end of each diagram, and the final state, with photon ω_s and phonon ω present, occurs on the right. It is possible to envisage more complicated processes connecting the initial and final states, but these are all of higher order and give a smaller contribution to the scattering. It is noted that processes 4 (*b*) and 4 (*c*) require the existence of infra-red-active phonons, and could therefore not take place in a homopolar crystal, e.g. diamond. Indeed, numerical estimates indicate that even when all three processes are allowed, 4 (*a*) dominates 4 (*b*) and 4 (*c*) in scattering intensity, and most theoretical work on Raman scattering has explicitly assumed that the radiation interacts with the lattice vibrations through the intermediary of the electrons in the crystal.

Expressed in words, process 4 (*a*) involves three virtual electronic transitions accompanied by the following photon and phonon transitions: (1) a photon ω_i is absorbed, (2) an optic phonon ω is created, (3) a photon ω_s is emitted. The scattering crystal is generally in its electronic ground state, with all valence bands full and all conduction bands empty, at the start of the scattering process, and it returns to its electronic ground state at the end of the event. The virtual intermediate states involve the excitation of electron–hole pairs. The three transitions can occur in any time order, leading to six related processes which could be illustrated by deforming fig. 4 (*a*) to change the relative order of the transition vertices.

The problem of calculating the scattering intensity due to the basic process 4 (*a*) has been tackled in a variety of ways. The first systematic treatment of optic-phonon Raman scattering in crystals was given by Born and Bradburn (1947) and the same approach has subsequently been used in further work by Born and his collaborators (Smith 1948, Theimer 1951, Born and Huang 1954). In this approach, which makes use of the semi-classical radiation theory, the intensity of the scattered radiation is arrived at by calculating the electric moment $\mathbf{M}$ set up in the crystal by the electric vector $\mathrm{Re}\,[\mathbf{E}\exp(-i\omega t)]$ of the incident light beam. If the polarizability tensor associated with the electrons in the crystal is $\alpha_{\rho\sigma}$, then

$$M_\rho = \sum_\sigma \alpha_{\rho\sigma} E_\sigma. \qquad (22)$$

The scattered light is produced by re-radiation of energy by the oscillating dipole moment $\mathbf{M}$, the scattered intensity being proportional to $|\mathbf{M}|^2$ and inversely proportional to the fourth power of the wavelength of the scattered light. The quantum-mechanical expression for the electronic polarizability tensor $\alpha_{\rho\sigma}$ involves the energy eigenvalues and wave-functions of the electron system (see Born and Huang 1954). Because of the existence of the electron-lattice interaction H_{EL}, the electronic eigenvalues and wave-functions in a diatomic lattice depend on the relative displacement amplitude $\mathbf{r}$ of the two sub-lattices, and the electronic polarizability can be expanded in a power series in $\mathbf{r}$:

$$\alpha_{\rho\sigma} = \alpha^{(0)}_{\rho\sigma} + \sum_\mu \alpha_{\rho\sigma,\mu} r_\mu + \sum_{\mu,\nu} \alpha_{\rho\sigma,\mu\nu} r_\mu r_\nu + \mathrm{O}(r^3), \qquad (23)$$

where

$$\alpha_{\rho\sigma,\mu} = \left(\frac{\partial \alpha_{\rho\sigma}}{\partial r_\mu}\right)_{r=0} \quad \text{and} \quad \alpha_{\rho\sigma,\mu\nu} = \left(\frac{\partial^2 \alpha_{\rho\sigma}}{\partial r_\mu \partial r_\nu}\right)_{r=0}. \qquad (24)$$

The term linear in r gives rise to the first-order Raman scattering, the quadratic term gives rise to second-order Raman scattering, and so on. The forms of the terms which occur in the expansion have been discussed by Born and Huang (1954).

The Born and Bradburn method has been applied to first-order Raman scattering in diamond by Smith (1948). The square of the relative displacement amplitude caused by a single optic phonon in diamond is given by (7):

$$\langle r^2 \rangle = \hbar / 2M\omega_0, \qquad (25)$$

where ω_0 is the optic phonon frequency. Consider the scattering geometry shown in fig. 5, where x, y and z are orthogonal axes which coincide with principal axes of the crystal and $\mathbf{k}_i$, $\mathbf{k}_s$ and $\mathbf{k}$ are the wave vectors of the incident light, scattered light and phonon respectively. Energy and wave vector conservation lead to:

$$\omega_i = \omega_s + \omega_0, \quad . \quad . \quad . \quad . \quad . \quad . \quad . \quad . \quad . \quad (26)$$

$$\mathbf{k}_i = \mathbf{k}_s + \mathbf{k}. \quad . \quad . \quad . \quad . \quad . \quad . \quad . \quad . \quad . \quad (27)$$

Since the percentage difference between ω_i and ω_s is small, $|\mathbf{k}_i|$ and $|\mathbf{k}_s|$ are not very different and they have been assumed equal in calculating the phonon direction. This approximation leads to:

$$k = 2k_i \sin(\psi/2). \quad . \quad . \quad . \quad . \quad . \quad . \quad . \quad . \quad (28)$$

Smith considers the case of right-angle scattering where $\psi = 90°$. We define the Raman scattering efficiency S to be the ratio of the number of scattered photons ω_s produced per unit time per unit cross-sectional area

Fig. 5

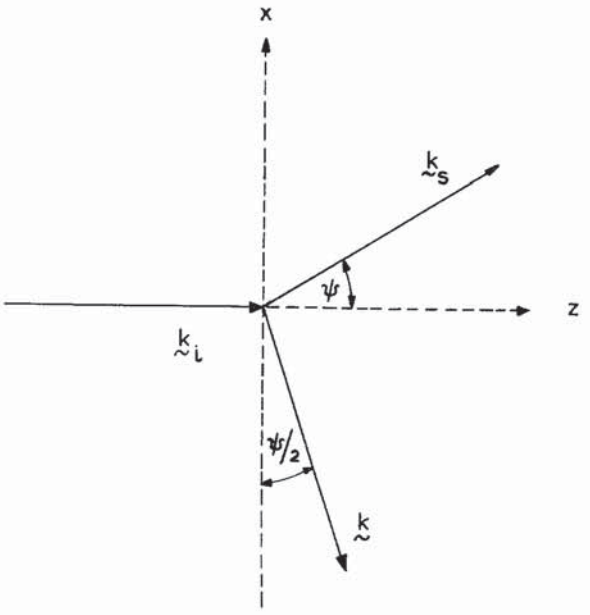

Raman scattering geometry.

of the crystal in solid angle $d\Omega$ about the direction of observation to the number of incident photons ω_i crossing unit area in unit time. Smith has investigated the symmetry properties of $\alpha_{\rho\sigma,\mu}$ and finds that the only non-vanishing components of the tensor are those for which ρ, σ and μ refer to different crystal axes. This leaves three distinct components (the tensor is symmetrical with respect to interchange of ρ and σ because it is derived from the symmetrical polarizability tensor $\alpha_{\rho\sigma}$) which are all equal.

The result of Smith for the first-order Raman scattering efficiency with unpolarized incident light and unanalysed scattered light is:

$$S = \frac{3\hbar\omega_s^4 L d\Omega}{\rho c^4 \omega_0} |\alpha_{zy,x}|^2 (n_0+1), \quad . \quad . \quad . \quad . \quad . \quad (29)$$

where L is the length of the crystal in the direction of $\mathbf{k}_i$, ρ is the crystal density and n_0 is the Bose population factor. The expression for the anti-Stokes component has n_0+1 replaced by n_0.

A more direct way of obtaining the Raman scattering tensor is to treat the three-step scattering process illustrated in fig. 4(*a*) by third-order time-dependent perturbation theory, and this calculation has been performed by Loudon (1963 b) for the particular cases of diamond and zinc blende structure crystals. In this approach, which uses second quantization of the radiative field, the quantity calculated is the probability per unit time $1/\tau$ that one of the incident photons is destroyed in a Raman scattering process, given by the usual third-order expression:

$$\frac{1}{\tau} = \frac{2\pi}{\hbar^6} \sum_{\mathbf{k},\mathbf{k}_s} \left| \sum_{a,b} \frac{\langle n_i - 1, 1; n_0+1; 0|H_I|a\rangle\langle a|H_I|b\rangle\langle b|H_I|n_i, 0; n_0; 0\rangle}{(\omega_a - \omega_i)(\omega_b - \omega_i)} \right|^2 \times \delta(\omega_i - \omega_0 - \omega_s), \quad . \quad . \quad . \quad . \quad . \quad . \quad . \quad (30)$$

where n_i, 0 and n_0 are the numbers of incident photons, scattered photons and optic phonons present in the initial state, a and b run over complete sets of intermediate states for the whole system, the summation over $\mathbf{k}_s$ includes only directions within the solid angle $d\Omega$, and $H_I = H_{ER} + H_{EL}$. The H_{ER} part contributes in two of the matrix elements while it is the H_{EL} part which contributes in the third matrix element. The final zeros in the initial and final state quantum numbers indicate that the electrons are in their ground state before and after the scattering event. Evaluating the summations and the matrix elements, (30) leads to the following expression for the scattering efficiency assuming the same geometry as Smith:

$$S = \frac{L\epsilon^{1/2}}{\tau n_i c} = \frac{e^4 \omega_s V (n_0+1) L d\Omega}{4\hbar^3 m^4 d^2 M c^4 \omega_0 \omega_i} [|R^x_{yz}|^2 + |R^z_{xy}|^2 + |R^y_{xz}|^2], \quad . \quad (31)$$

where e and m are the electronic charge and mass, d is the lattice constant and V is the crystal volume. The three components of the tensor R are equal for diamond or zinc blende structure crystals, and are given by expressions of the form:

$$R^x_{yz} = R^x_{yz}(-\omega_i, \omega_s, \omega_0) = \frac{1}{V} \sum_{\alpha,\beta} \left\{ \frac{p^z_{0\beta} \Xi^x_{\beta\alpha} p^y_{\alpha 0}}{(\omega_\beta + \omega_0 - \omega_i)(\omega_\alpha - \omega_i)} + \text{five similar terms} \right\}, \quad . \quad (32)$$

where the subscripts on the p and Ξ matrix elements refer to electron–hole pair states with energies $\hbar\omega_\alpha$ and $\hbar\omega_\beta$, 0 referring to the electronic ground state. The two subscripts on R are the polarization directions of the incident and scattered photons respectively while the superscript is the

direction of polarization of the phonon. The explicit term on the right-hand side of (32) arises from the order of interaction vertices drawn in fig. 4(*a*), and the remaining five terms correspond to the other possible diagrams obtainable by rearrangement of this order. The two matrix elements of the electronic momentum operator p arises from the two H_{ER} matrix elements. The electron–lattice interaction H_{EL} has been treated in the deformation potential approximation (Bir and Pikus 1961, Whitfield 1961) and the Ξ matrix elements are deformation potentials.

The signs attached to the frequencies in R^x_{yz} on the right-hand side of (32) have been chosen so that a negative (positive) frequency corresponds to destruction (creation) of the appropriate photon or phonon. Whereas the analogous quantity $\alpha_{\rho\sigma,\mu}$ used in the Born theory of Raman scattering was invariant under interchange of the polarizations ρ and σ of the scattered and incident photons, R^x_{yz} does not in general have the corresponding property. Instead, inspection of the complete form of the tensor shows that it satisfies:

$$R^x_{yz}(-\omega_{\mathrm{i}}, \omega_{\mathrm{s}}\, \omega_0) = R^x_{zy}(-\omega_{\mathrm{i}} + \omega_0, \omega_{\mathrm{s}} + \omega_0, -\omega_0). \quad . \quad . \quad (33)$$

However, when ω_0 is sufficiently small that it can be neglected in comparison with all the other frequencies occurring in the tensor, as is usually the case, (33) becomes:

$$R^x_{yz}(-\omega_{\mathrm{i}}, \omega_{\mathrm{i}}, 0) = R^x_{zy}(-\omega_{\mathrm{i}}, \omega_{\mathrm{i}}, 0) \quad . \quad . \quad . \quad (34)$$

and R^x_{yz} has the same symmetry properties as $\alpha_{zy,\,x}$. Indeed, explicit calculation of $\alpha_{zy,\,x}$ using the deformation potential electron–lattice interaction and the well-known quantum-mechanical form of the polarizability tensor, gives:

$$\alpha_{zy,\,x} = -\frac{e^2}{m^2\omega_{\mathrm{i}}^2\hbar^2 d}\, R^x_{yz}(-\omega_{\mathrm{i}}, \omega_{\mathrm{i}}, 0). \quad . \quad . \quad . \quad . \quad (35)$$

Thus for diamond, where $\rho = 4M/V$, (29) and (31) become identical in the small ω_0 limit. Numerical estimates based on (31) indicate that Raman scattering efficiencies may typically be of order 10^{-6} or 10^{-7}.

The interaction H_{ER} between the radiation, having electric field $\mathbf{E}$ and vector potential $\mathbf{A}$, and the electrons, having position $\mathbf{x}$ and momentum $\mathbf{p}$, can be represented either as $-e\mathbf{E}.\mathbf{x}$ or as $-e\mathbf{A}.\mathbf{p}/mc$. For Raman scattering from molecules, both representations lead to the same results for the scattering tensor, contrary to an assertion by Kondilenko *et al.* (1960) (see the correction by Kondilenko and Strizhevskii 1961). However, for scattering by crystals the matrix elements of $\mathbf{x}$ have complicated properties due to the fact that the electronic wave functions extend throughout the crystal (see Blount 1963 and the conclusion of Butcher and McLean 1963) and it is more satisfactory to use the $-e\mathbf{A}.\mathbf{p}/mc$ representation, even though this leads to formulae which do not explicitly show the dependence of the scattered intensity on the fourth power of the wavelength (cf. (29), (31) and (35)).

Strizhevskii (1962) has considered the theory of Raman scattering in non-cubic crystals. He treats the quantization of the radiative field in

Raman-active vibrational symmetries and Raman tensors for the crystal symmetry classes

System	Class		Raman tensors			
Monoclinic			$\begin{pmatrix} a & d \\ & b \\ d & c \end{pmatrix}$	$\begin{pmatrix} & e \\ e & & f \\ & f \end{pmatrix}$		
	2	C_2	$A(y)$	$B(x, z)$		
	m	C_s	$A'(x, z)$	$A''(y)$		
	2/m	C_{2h}	A_g	B_g		
Orthorhombic			$\begin{pmatrix} a & & \\ & b & \\ & & c \end{pmatrix}$	$\begin{pmatrix} & d & \\ d & & \\ & & \end{pmatrix}$	$\begin{pmatrix} & & e \\ & & \\ e & & \end{pmatrix}$	$\begin{pmatrix} & & \\ & & f \\ & f & \end{pmatrix}$
	222	D_2	A	$B_1(z)$	$B_2(y)$	$B_3(x)$
	mm2	C_{2v}	$A_1(z)$	A_2	$B_1(x)$	$B_2(y)$
	mmm	D_{2h}	A_g	B_{1g}	B_{2g}	B_{3g}
Trigonal			$\begin{pmatrix} a & & \\ & a & \\ & & b \end{pmatrix}$	$\begin{pmatrix} c & d & e \\ d & -c & f \\ e & f & \end{pmatrix}$	$\begin{pmatrix} d & -c & -f \\ -c & -d & e \\ -f & e & \end{pmatrix}$	
	3	C_3	$A(z)$	$E(x)$	$E(y)$	
	$\bar{3}$	C_{3i}	A_g	E_g	E_g	
			$\begin{pmatrix} a & & \\ & a & \\ & & b \end{pmatrix}$	$\begin{pmatrix} c & & \\ & -c & d \\ & d & \end{pmatrix}$	$\begin{pmatrix} & -c & -d \\ -c & & \\ -d & & \end{pmatrix}$	
	32	D_3	A_1	$E(x)$	$E(y)$	
	3m	C_{3v}	$A_1(z)$	$E(y)$	$E(-x)$	
	$\bar{3}$m	D_{3d}	A_{1g}	E_g	E_g	

Tetragonal			$\begin{pmatrix} a & & \\ & a & \\ & & b \end{pmatrix}$	$\begin{pmatrix} c & d & \\ d & -c & \\ & & \end{pmatrix}$	$\begin{pmatrix} & & e \\ & & f \\ e & f & \end{pmatrix}$	$\begin{pmatrix} & & -f \\ & & e \\ -f & e & \end{pmatrix}$				
	$\bar{4}$	C_4	$A(z)$	B	$E(x)$	$E(y)$				
	$\bar{4}$	S_4	A	$B(z)$	$E(x)$	$E(-y)$				
	4/m	C_{4h}	A_g	B_g	E_g	E_g				
			$\begin{pmatrix} a & & \\ & a & \\ & & b \end{pmatrix}$	$\begin{pmatrix} c & & \\ & -c & \\ & & \end{pmatrix}$	$\begin{pmatrix} & d & \\ d & & \\ & & \end{pmatrix}$	$\begin{pmatrix} & & e \\ & & \\ e & & \end{pmatrix}$	$\begin{pmatrix} & & \\ & & e \\ & e & \end{pmatrix}$			
	4mm	C_{4v}	$A_1(z)$	B_1	B_2	$E(x)$	$E(y)$			
	422	D_4	A_1	B_1	B_2	$E(-y)$	$E(x)$			
	$\bar{4}$2m	D_{2d}	A_1	B_1	$B_2(z)$	$E(y)$	$E(x)$			
	4/mmm	D_{4h}	A_{1g}	B_{1g}	B_{2g}	E_g	E_g			
Hexagonal			$\begin{pmatrix} a & & \\ & a & \\ & & b \end{pmatrix}$	$\begin{pmatrix} & & c \\ & & d \\ c & d & \end{pmatrix}$	$\begin{pmatrix} & & -d \\ & & c \\ -d & c & \end{pmatrix}$	$\begin{pmatrix} e & f & \\ f & -e & \\ & & \end{pmatrix}$	$\begin{pmatrix} f & -e & \\ -e & -f & \\ & & \end{pmatrix}$			
	6	C_6	$A(z)$	$E_1(x)$	$E_1(y)$	E_2	E_2			
	$\bar{6}$	C_{3h}	A'	E''	E''	$E'(x)$	$E'(y)$			
	6/m	C_{6h}	A_g	E_{1g}	E_{1g}	E_{2g}	E_{2g}			
			$\begin{pmatrix} a & & \\ & a & \\ & & b \end{pmatrix}$	$\begin{pmatrix} & & c \\ & & \\ c & & \end{pmatrix}$	$\begin{pmatrix} & & -c \\ & & \\ -c & & \end{pmatrix}$	$\begin{pmatrix} & d & \\ d & & \\ & & \end{pmatrix}$	$\begin{pmatrix} d & & \\ & -d & \\ & & \end{pmatrix}$			
	622	D_6	A_1	$E_1(x)$	$E_1(y)$	E_2	E_2			
	6mm	C_{6v}	$A_1(z)$	$E_1(y)$	$E_1(-x)$	E_2	E_2			
	$\bar{6}$m2	D_{3h}	A_1'	E''	E''	$E'(x)$	$E'(y)$			
	6/mmm	D_{6h}	A_{1g}	E_{1g}	E_{1g}	E_{2g}	E_{2g}			
Cubic			$\begin{pmatrix} a & & \\ & a & \\ & & a \end{pmatrix}$	$\begin{pmatrix} b & & \\ & b & \\ & & b \end{pmatrix}$	$\begin{pmatrix} b & & \\ & b & \\ & & b \end{pmatrix}$	$\begin{pmatrix} & & \\ & & d \\ & d & \end{pmatrix}$	$\begin{pmatrix} & & d \\ & & \\ d & & \end{pmatrix}$	$\begin{pmatrix} & d & \\ d & & \\ & & \end{pmatrix}$		
	23	T	A	E	E	$F(x)$	$F(y)$	$F(z)$		
	m3	T_h	A_g	E_g	E_g	F_g	F_g	F_g		
	432	O	A_1	E	E	F_2	F_2	F_2		
	$\bar{4}$3m	T_d	A_1	E	E	$F_2(x)$	$F_2(y)$	$F_2(z)$		
	m3m	O_h	A_{1g}	E_g	E_g	F_{2g}	F_g	F_{2g}		

an anisotropic crystal and derives a formula for the scattered light intensity which is sufficiently general in form to apply to scattering by phonons, impurities, lattice defects, etc. As a result of this generality it is difficult to draw any explicit conclusions from his formula.

2.3. *Selection Rules and the Symmetry of the Scattered Light*

The different long-wavelength phonon branches in a given crystal correspond to different symmetries of vibration of the atoms in the unit cell and are characterized by irreducible representations of the space group of the crystal lattice. If the wavelengths of the Raman phonons are assumed to be effectively infinite, then the crystal point group can be used in classifying the phonon symmetries. This infinite wavelength assumption is not valid for Raman-active phonons which are also infra-red active, as is evident from the discussion of § 2.1, and this type of vibration will be discussed separately in the following section.

The selection rules for Raman-active phonons can be determined by standard group-theoretical methods and the calculation is described in some detail by Heine (1960), who bases his work on the polarizability derivative theory of Born and Bradburn (1947) described in the previous section (see also Theimer 1953). The result of this approach is that a phonon can participate in a first-order Raman transition if and only if its irreducible representation is the same as one of the irreducible representations which occur in the reduction of the representation of the polarizability tensor. The irreducible representations by which the components of the polarizability tensor transform are conveniently listed by Herzberg (1945) and Wilson *et al.* (1955) for the set of molecular point groups, which includes the 32 crystal point groups. Mathieu (1945) has listed the Raman-active vibrational symmetries for the different crystal classes. Many of the results had been given at an earlier date by Bhagavantam and Venkatarayudu (1939) who considered several particular crystals in detail.

The intensity of the Raman-scattered radiation depends in general on the directions of observation and illumination relative to the principal axes of the crystal. The angular variation of the scattering gives information about the symmetry of the lattice vibration responsible. The anisotropy of the scattering can be predicted for a vibration of any given symmetry by standard group-theoretical methods or by simple symmetry arguments not using group theory directly (Saksena 1940, Mathieu 1945, Ovander 1960).

The results of all the above authors, with several errors corrected, are collected together in the table. Opposite each crystal class are listed the irreducible representations of the Raman-active lattice vibrations, using the notation of Herzberg (1945) and Wilson *et al.* (1955) for the irreducible representations (other authors sometimes have slightly different notations). Where an x, y or z occurs in brackets after an irreducible representation, this indicates that the vibration is also infra-red active and has the direction of polarization indicated. Such vibrations, which occur only in piezoelectric crystals (i.e. crystals with no centre of inversion symmetry) require